# Simultaneous compression, characterization and phase stabilization of GW-level 1.4 cycle VIS-NIR femtosecond pulses using a single dispersion-scan setup

**Francisco Silva,[1,*] Miguel Miranda,[1,2] Benjamín Alonso,[1,3] Jens Rauschenberger,[4] Vladimir Pervak,[4,5] and Helder Crespo[1]**

[1]*IFIMUP-IN and Departamento de Física e Astronomia, Faculdade de Ciências, Universidade do Porto, Rua do Campo Alegre 687, 4169-007 Porto, Portugal*
[2]*Department of Physics, Lund University, P.O. Box 118, SE-221 00 Lund, Sweden*
[3]*Universidad de Salamanca, Grupo de Investigación en Óptica Extrema (GIOE), Pl. de la Merced s/n E-37008 Salamanca, Spain*
[4]*UltraFast Innovations GmbH, Am Coulombwall 1, 85748 Garching, Germany*
[5]*Ludwig-Maximilians-Universität München, Department für Physik, Am Coulombwall 1, 85748 Garching, Germany*
[*]*fsilvaportugal@gmail.com*

**Abstract:** We have temporally characterized, dispersion compensated and carrier-envelope phase stabilized 1.4-cycle pulses (3.2 fs) with 160 μJ of energy at 722 nm using a minimal and convenient dispersion-scan setup. The setup is all inline, does not require interferometric beamsplitting, and uses components available in most laser laboratories. Broadband minimization of third-order dispersion using propagation in water enabled reducing the compressed pulse duration from 3.8 to 3.2 fs with the same set of chirped mirrors. Carrier-envelope phase stabilization of the octave-spanning pulses was also performed by the dispersion-scan setup. This unprecedentedly simple and reliable approach provides reproducible CEP-stabilized pulses in the single-cycle regime for applications such as CEP-sensitive spectroscopy and isolated attosecond pulse generation.



**OCIS codes:** (320.2250) Femtosecond phenomena; (320.5520) Pulse compression; (320.7090) Ultrafast lasers; (320.7100) Ultrafast measurements.

## References and links

1. F. Krausz, "Attosecond physics," Rev. Mod. Phys. **81**(1), 163–234 (2009).
2. A. H. Zewail, "Femtochemistry: Atomic-scale dynamics of the chemical bond," Angew. Chem. Int. Ed. Engl. **39**(15), 2586–2631 (2000).
3. P. H. Bucksbaum, "The future of attosecond spectroscopy," Science **317**(5839), 766–769 (2007).
4. M. Hentschel, R. Kienberger, C. Spielmann, G. A. Reider, N. Milosevic, T. Brabec, P. Corkum, U. Heinzmann, M. Drescher, and F. Krausz, "Attosecond metrology," Nature **414**(6863), 509–513 (2001).
5. E. Goulielmakis, Z.-H. Loh, A. Wirth, R. Santra, N. Rohringer, V. S. Yakovlev, S. Zherebtsov, T. Pfeifer, A. M. Azzeer, M. F. Kling, S. R. Leone, and F. Krausz, "Real-time observation of valence electron motion," Nature **466**(7307), 739–743 (2010).
6. S. Adachi, N. Ishii, Y. Nomura, Y. Kobayashi, J. Itatani, T. Kanai, and S. Watanabe, "1.2 mJ sub-4-fs source at 1 kHz from an ionizing gas," Opt. Lett. **35**(7), 980–982 (2010).
7. C. Manzoni, S.-W. Huang, G. Cirmi, P. Farinello, J. Moses, F. X. Kärtner, and G. Cerullo, "Coherent synthesis of ultra-broadband optical parametric amplifiers," Opt. Lett. **37**(11), 1880–1882 (2012).
8. T. Witting, F. Frank, C. A. Arrell, W. A. Okell, J. P. Marangos, and J. W. Tisch, "Characterization of high-intensity sub-4-fs laser pulses using spatially encoded spectral shearing interferometry," Opt. Lett. **36**(9), 1680–1682 (2011).
9. E. Goulielmakis, M. Schultze, M. Hofstetter, V. S. Yakovlev, J. Gagnon, M. Uiberacker, A. L. Aquila, E. M. Gullikson, D. T. Attwood, R. Kienberger, F. Krausz, and U. Kleineberg, "Single-cycle nonlinear optics," Science **320**(5883), 1614–1617 (2008).
10. A. Wirth, M. T. Hassan, I. Grguraš, J. Gagnon, A. Moulet, T. T. Luu, S. Pabst, R. Santra, Z. A. Alahmed, A. M. Azzeer, V. S. Yakovlev, V. Pervak, F. Krausz, and E. Goulielmakis, "Synthesized light transients," Science **334**(6053), 195–200 (2011).

#205337 - $15.00 USD Received 23 Jan 2014; revised 14 Mar 2014; accepted 25 Mar 2014; published 21 Apr 2014

11. M. Miranda, T. Fordell, C. Arnold, A. L'Huillier, and H. Crespo, "Simultaneous compression and characterization of ultrashort laser pulses using chirped mirrors and glass wedges," Opt. Express **20**(1), 688–697 (2012).
12. A. Baltuska, M. S. Pshenichnikov, and D. A. Wiersma, "Second-harmonic generation frequency-resolved optical gating in the single-cycle regime," IEEE J. Quantum Electron. **35**(4), 459–478 (1999).
13. B. Alonso, M. Miranda, Í. J. Sola, and H. Crespo, "Spatiotemporal characterization of few-cycle laser pulses," Opt. Express **20**(16), 17880–17893 (2012).
14. M. Miranda, C. L. Arnold, T. Fordell, F. Silva, B. Alonso, R. Weigand, A. L'Huillier, and H. Crespo, "Characterization of broadband few-cycle laser pulses with the d-scan technique," Opt. Express **20**(17), 18732–18743 (2012).
15. B. Alonso, M. Miranda, F. Silva, V. Pervak, J. Rauschenberger, J. San Román, Í. J. Sola, and H. Crespo, "Characterization of sub-two-cycle pulses from a hollow-core fiber compressor in the spatiotemporal and spatiospectral domains," Appl. Phys. B **112**(1), 105–114 (2013).
16. D. J. Jones, S. A. Diddams, J. K. Ranka, A. Stentz, R. S. Windeler, J. L. Hall, and S. T. Cundiff, "Carrier-envelope phase control of femtosecond mode-locked lasers and direct optical frequency synthesis," Science **288**(5466), 635–639 (2000).
17. V. Pervak, I. Ahmad, M. K. Trubetskov, A. V. Tikhonravov, and F. Krausz, "Double-angle multilayer mirrors with smooth dispersion characteristics," Opt. Express **17**(10), 7943–7951 (2009).
18. A. Suda and T. Takeda, "Effects of nonlinear chirp on the self-phase modulation of ultrashort optical pulses," Appl. Sciences **2**(4), 549–557 (2012).
19. Y. Coello, B. Xu, T. L. Miller, V. V. Lozovoy, and M. Dantus, "Group-velocity dispersion measurements of water, seawater, and ocular components using multiphoton intrapulse interference phase scan," Appl. Opt. **46**(35), 8394–8401 (2007).

## 1. Introduction

High peak power laser pulses with single-cycle durations are increasingly sought after due to their potential for strong field physics [1] and ultrafast spectroscopy studies [2,3]. Ironically, the correct measurement of these pulses is as much of a problem as their generation, since such broadband sources require a significant amount of optimization, which is unfeasible without reliable diagnostics. Without a sufficiently sensitive and precise measurement technique it is actually impossible to characterize the performance of the source. For the last 30 years significant work has been done in femtosecond pulse measurement, where reliable techniques were invented and studied. These have led to many significant advances in several fields, most notably in strong field physics, including the generation of attosecond pulses [4] and the observation of valence electron motion [5]. In the sub-1.5-cycle regime, techniques such as FROG [6], SPIDER [7,8] and attosecond streaking [9] have been used to measure pulses down to 0.88 cycles in duration [10]. Despite their success, such techniques employ setups with numerous optical elements, often requiring interferometric beamsplitting and recombination (in the case of streaking the requirements are even higher – one needs a working attosecond beamline to provide the shorter temporal gate pulse). This complexity translates into additional alignment and calibration time, which reduces the usefulness of the technique. It is therefore interesting to investigate simpler, more straightforward ways to accomplish the same task. Recently, we demonstrated a new technique dubbed dispersion-scan (or d-scan), whose experimental implementation is straightforward, only requiring the addition of a second-harmonic generation (SHG) stage with sufficient bandwidth to the standard chirped mirror compressor employed to manage dispersion throughout the experimental setup [11]. The principle behind d-scan is to monitor the generated SHG spectrum as a function of dispersion around the optimum compression point and using this information, together with a measurement of the pulse spectrum, to retrieve the spectral phase, thereby fully characterizing the pulse temporally. Furthermore, the retrieval algorithm is robust regarding bandwidth limitations in the nonlinear process used, eliminating the source of one of the most common systematic errors that plagues few-cycle pulse measurement [12]. To this date, d-scan has been demonstrated with few-cycle laser oscillators [11,13,14] and a high energy hollow-fiber compressor yielding 4.5 fs pulses [15].

In this work we demonstrate the feasibility to use d-scan in the sub-1.5-cycle regime by characterizing 1.4-cycle/3.2 fs pulses generated in a hollow fiber compressor, with dispersion compensation performed using state-of-the-art octave-spanning chirped mirrors. The setup was composed of the usual chirped mirror compressor with glass wedges for dispersion fine-

#205337 - $15.00 USD Received 23 Jan 2014; revised 14 Mar 2014; accepted 25 Mar 2014; published 21 Apr 2014

tuning, plus a SHG stage to monitor the SHG spectrum of the pulse as a function of dispersion. This setup, besides being able to both compress and characterize the pulses temporally, also doubles as an f-2f interferometer [16] when the laser spectrum is octave-spanning. As such, we also demonstrate that one can use it to monitor and stabilize the CEP jitter of the pulses, achieving a stability of 140 mrad over 100 minutes.

One difficulty encountered during this study concerns the limited flexibility of chirped mirror compressors – their phase is essentially fixed, except for the variable glass thickness introduced by the wedge pair. This allows one to optimize the pulse phase unidimensionally, and for the case where the compensated phase matches the nonlinear plus propagation phase perfectly, one achieves perfect compression for a certain glass thickness. For situations where the phase to be compensated for does not match the target phase of the chirped mirror compressor, one will still be able to have zero GDD at a certain wavelength but not across the whole spectrum, i.e., there might be a significant amount of higher order phase, most commonly TOD. When working with near-single cycle pulses this can affect the result greatly as an apparently small amount of TOD over a large spectrum can significantly increase the pulse duration, decrease the peak power and create satellite pulses. Hence it would be desirable to be able to tune the final TOD of the pulse without having to resort to a new set of chirped mirrors. One possible way to achieve this would be by changing the fine-tuning element (e.g., glass wedges) to a material with an exactly symmetric dispersion with respect to the rest of the experimental setup, which is not always possible, as there exists only a limited number of materials, each with its specific dispersion curve. In this work we found that in cases of excessive negative TOD in the VIS-NIR range one can exchange propagation through glass to propagation through water to increase the amount of positive TOD in the pulse, leading to considerably better performance in the case of our compressor. We have demonstrated a reduction of pulse duration from 3.8 to 3.2 fs, accompanied by a significant improvement in pulse contrast and peak intensity.

## 2. Experimental

### *2.1 Laser source*

Our laser system is composed of a CPA Ti:Sapphire amplifier (Femtolasers FemtoPower Compact PRO) seeded by pulses from a broadband few-cycle CEP-stabilized prismless Ti:Sa oscillator (Femtolasers Rainbow) temporally stretched in bulk glass. The amplifier features a prism compressor and chirped mirrors for TOD precompensation before amplification, delivering 33 fs pulses (intensity FWHM) with up to 850 μJ at 1 kHz. While the spectrum of the amplifier is sufficient to support 24 fs pulses, there is significant uncompensated residual phase due to sub-optimal TOD precompensation and self-phase modulation in the prisms. We found this not to be a limiting factor regarding the generation of compressible octave-spanning spectra.

The output from the amplifier is focused by a f = 1.5 m lens into a 1 m long, 250 μm hollow-core fiber (HF) containing Argon at 1 atm of pressure. Spatial coupling into the fiber is optimized using an iris placed before the lens, transmitting roughly 400 μJ out of 580 μJ. After propagation through the fiber and output window, the beam contains 200 μJ, corresponding to 50% transmission, with a typical RMS power stability of 0.5% over 1 hour.

### *2.2 Dispersion scan*

A schematic of the dispersion scan setup is represented in Fig. 1. The beam is collimated with an f = 1.25 m silver mirror and then sent through a pair of antireflection (AR) coated (650-1050 nm) 8 degree BK7 wedges that constitute the variable dispersion element of the d-scan setup, as well as the feedback element for the CEP slow-loop. These two tasks have different requirements, though: for d-scan one needs a fast stage (>5 mm/s) with coarse resolution (~10 μm steps); for CEP feedback one needs a high-resolution stage with fast response time. We found that it is less expensive to have a different stage in each wedge, each optimized for a particular task. For d-scan we mounted one of the wedges in a linear motion guide coupled to

#205337 - $15.00 USD Received 23 Jan 2014; revised 14 Mar 2014; accepted 25 Mar 2014; published 21 Apr 2014

a stepper motor using a trapezoidal leadscrew, encoded with a slide encoder with 140 µm resolution, which due to the small angle of the wedges results in a 20 µm glass insertion resolution. For CEP feedback we mounted the second wedge on a Newport AG-LS25 piezo motor driven stage, capable of fast, ripple-free, no backlash, high-precision motion. The beam is then compressed in a double-angle chirped mirror compressor (Ultrafast Innovations GmbH), designed to compensate propagation through 1 m of air and 1 mm of fused silica from 500 nm to 1050 nm for every 2 bounces. The reflectivity bandwidth of the mirrors extends down to 450 nm, exhibiting a sharp cutoff at this wavelength. After ten bounces, half at 5 degrees incidence angle and half at 19 degrees, a small percentage of the beam is reflected by a small angle wedge for the dispersion-scan measurement. The transmitted beam is free to be used in experiments, containing 160 µJ.

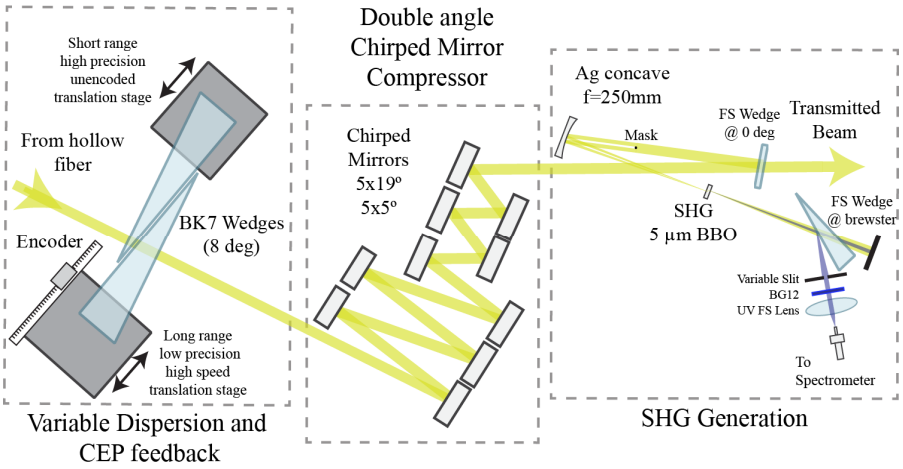


Fig. 1. Schematic of the d-scan setup.

The central part of the reflected beam is blocked by a thin wire for later separation of the SHG and fundamental beams [14] and is then focused by a f = 250 mm concave silver mirror into a 5 µm thick BBO crystal cut for type-I SHG at 800 nm, generating a broadband SHG signal in the s-polarization plane (this signal can in fact be seen as sum-frequency generation, SFG, resulting from the convolution of the fundamental spectrum with itself, whose shape and intensity strongly depends on the spectral phase [11]). To retain only this s-polarization signal, a reflection from an uncoated fused silica wedge oriented at Brewster's angle reflects 12% of s-polarization and a residual amount of p-polarization, effectively serving as a broadband polarizer. Most of the remaining fundamental is then cut by a variable slit and a BG12 filter is added to further improve rejection of the fundamental. The resulting beam is then coupled into a spectrometer (HR4000, Ocean Optics), intensity calibrated from 200 to 1100 nm by the manufacturer. By measuring the SHG/SFG spectrum as a function of BK7 propagation thickness, the experimental d-scan trace is recorded. The total BK7 range used for this study was 4.2 mm, corresponding to a total of 210 spectra at 20 µm steps. A complete trace is typically acquired in 10-30 seconds, depending on the integration time and stage speed used. The experimental trace, together with the measured fundamental spectrum, is used to retrieve the spectral phase using an algorithm based on the one described in [11,14], although in the present study a different kind of bootstrap method was employed: 5 d-scan traces were measured successively and retrieved independently, and statistics were done on the 5 retrieved spectral phases. This way, the uncertainty will include the sensitivity of the algorithm to experimental noise. Each retrieval takes about 1 minute in a state-of-the art workstation.

As discussed in [11,14], a common problem when characterizing such broad spectra is the bandwidth of the nonlinear process employed. In fact, even the bandwidth of a 5 µm BBO crystal would be narrow for these pulses. Still, there is no need for calibration and marginals,

#205337 - $15.00 USD Received 23 Jan 2014; revised 14 Mar 2014; accepted 25 Mar 2014; published 21 Apr 2014

since we can introduce a smooth response function in the retrieval, as discussed in [11], and the algorithm correctly converges to the correct phase and response function pair.

## 3. Experimental results

In the process of optimizing our pulse compression setup we have encountered several challenges that prevented us from directly attaining the 1.4-cycle regime. In hindsight, these problems are easily identifiable just by glancing at the d-scan traces. In this section we will illustrate the steps we have taken to overcome them.

### *3.1 Hollow fiber compressor*

A typical spectrum of the beam after the hollow fiber compressor and the chirped mirrors is shown in Fig. 2(a) (dashed line). At −10 dB, this spectrum spans from 450 nm to 1020 nm and supports a 2.9 fs pulse. Considering only the frequencies that the chirped mirror compressor can actually compress (500-1050 nm), it would support a 3.2 fs pulse. The repeatability of these parameters in day-to-day operation is surprisingly good: although the exact position and amplitude of the central peaks can change every time the fiber is realigned, the span and transform-limit of the spectrum is extremely consistent. As studied in a previous work, a wavelength dependence on mode size is present on the collimated beam (as expected from diffraction), which does not translate to spatio-temporal structure in the focus [15].

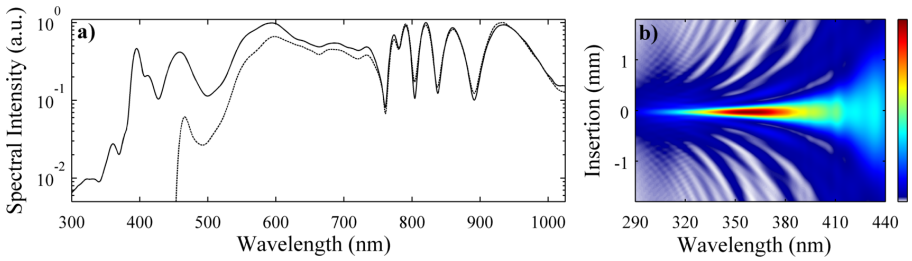


Fig. 2. (a) Black line: Typical spectrum generated in the HF compressor, supporting a 1.9 fs pulse at 690 nm. Dashed line: Typical spectrum, after propagation through the wedges and the chirped mirrors, supporting a 2.9 fs pulse at 722 nm. (b) Theoretical d-scan trace calculated from the spectrum in (a) (dashed line) and assuming a flat spectral phase.

The calculated d-scan trace corresponding to a perfectly compensated spectral phase is given in Fig. 2(b), where we see that all frequencies in the main peak of the pulse are compressed for the same wedge insertion; the maximum of the SHG signal provides the reference (zero) wedge insertion. Any deviation from this horizontal, smooth, flat shape then corresponds to uncompensated spectral phase, where different parts of the spectrum will be compressed for different insertions, hence giving a different SHG/SFG signal.

### *3.2 Double-angle chirped mirror alignment*

Double-angle chirped mirrors have the advantage over double-chirped mirror pairs that their manufacture requires only one coating-run [17], hence eliminating potential mismatches between independent batches. In contrast, they need to be used at two fixed incidence angles for which the corresponding GDD oscillations will have opposite phase and cancel each other out. If these two angles are not properly matched, residual oscillations can remain that will result in deficient compression, namely in a reduction of the peak intensity of the main pulse. As theoretically exemplified in [11], these oscillations show up as fringes in the dispersion-scan trace.

In order to better distinguish the fringes from the actual chirped mirror compressor from those caused by the nonlinear phase introduced by propagation in the hollow core fiber, we resorted to using a source with a known smooth spectral phase, namely the few-cycle oscillator studied in [11,13]. After an initial alignment of the chirped mirror compressor, where the angles were adjusted to within ± 2 degrees, it was obvious from the fringes present

#205337 - $15.00 USD Received 23 Jan 2014; revised 14 Mar 2014; accepted 25 Mar 2014; published 21 Apr 2014

in the d-scan traces that this precision was not enough (Fig. 3(a)). After a much more precise alignment we were able to reduce these fringes to a minimum (Fig. 3(b)).

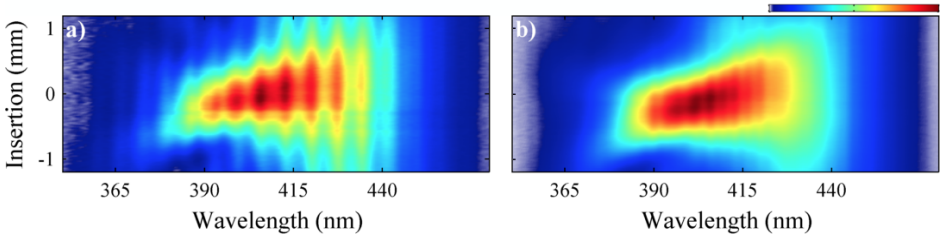


Fig. 3. (a) Measured d-scan trace of a few-cycle laser oscillator with a smooth spectral phase, as used in [11], with mirror angles adjusted to within ± 2 degrees. (b) The same measurement, after tweaking the chirped mirror angles to minimize residual phase oscillations.

### *3.3 Influence of the input phase*

As thoroughly studied [18], the input phase into a hollow fiber compressor has a great influence on the output phase, hence the input phase has to be carefully optimized to yield the best compressible phase at the output of the spectral broadening stage.

As theoretically demonstrated in [11], characteristic features in the d-scan trace have an explicit meaning: the vertical position of the trace (0th order) corresponds to GDD mismatch, i.e., if the trace moves for the same insertion range it means the GDD out of the hollow fiber has changed; a more pronounced tilt in the trace (1st order) corresponds to more TOD, and the sign of the tilt gives us the TOD signal; curvature in the trace corresponds to higher orders of dispersion; as explained in the last subsection, fringes in the d-scan trace correspond to very high orders of dispersion, i.e., phase oscillations.

In the present work we have verified that the input phase of the hollow fiber compressor has a strong nonlinear influence on the phase of the output pulse and has to be carefully optimized to achieve the flattest phase. In fact, as the input phase is varied using the amplifier prism compressor, the TOD affecting the output pulse goes through a minimum (Fig. 4), which in general we have found not to be correlated with the broadest achievable spectrum.

Still, the optimization procedure for achieving the flattest possible phase is straightforward – by measuring successive d-scans for several prism insertions one can easily find the position that minimizes the observed tilt in the traces, i.e., that minimizes the output TOD, which is essential to have the best compression.

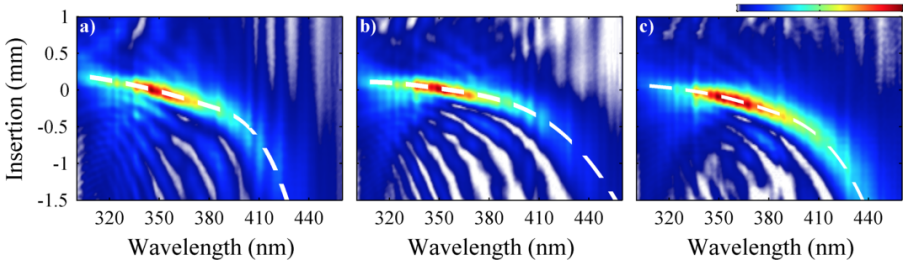


Fig. 4. (a) to (c) d-scans for increasing prism insertion in the prism compressor. The tilt of the high intensity part of the trace goes through a minimum, as shown in (b), corresponding to minimum TOD and best overall compression.

### *3.4 Pulse compression*

After optimizing the CPA compressor prism position for best compression after the hollow fiber we were, however, not able to achieve a pulse completely free of residual TOD. One can hypothesize that this is caused by at least one of three factors: 1) the phase of the chirped mirrors is not adequate for perfect compression of the hollow fiber output, possibly due to

#205337 - $15.00 USD Received 23 Jan 2014; revised 14 Mar 2014; accepted 25 Mar 2014; published 21 Apr 2014

manufacturing limitations; 2) due to different parameters used in this work, the optimum output phase has a final TOD different than the one the chirped mirrors were designed for; 3) the control over higher dispersion orders in the Ti:Sa amplifier is insufficient for full optimization of the output phase of the HF compressor, i.e., there is no fine control over all orders, as changing the prism position changes GDD and TOD at the same time. A CPA system incorporating a pulse shaper would in principle be able to do such fine optimizations but was not available for this work. The duration of the compressed pulse is nevertheless sub-2-cycle, as shown experimentally in Fig. 5. The retrieved pulse has an intensity FWHM of 3.8 ± 0.1 fs, which corresponds to 1.6 cycles at 722 nm.

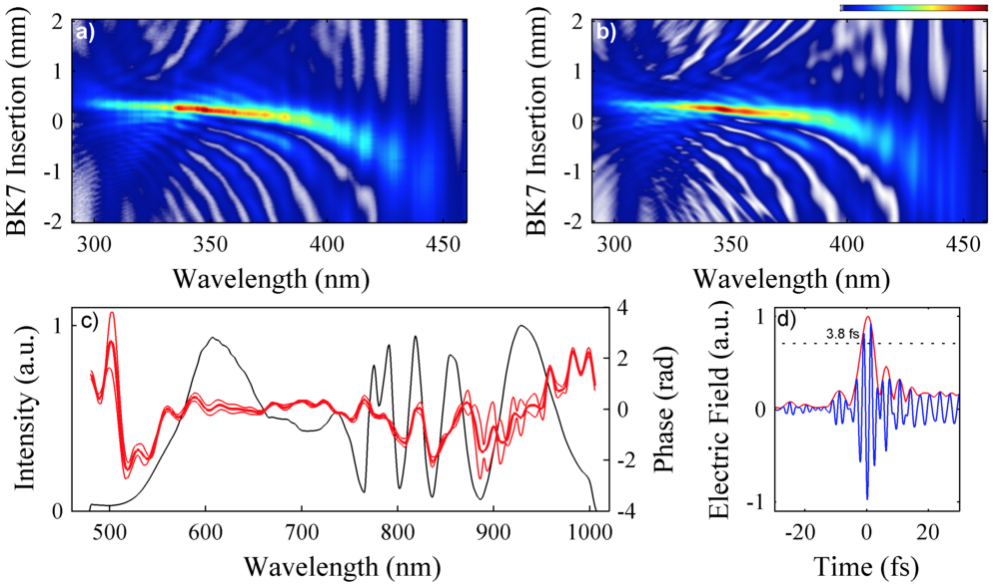


Fig. 5. Representative measured (a) and retrieved (b) d-scans for the setup in Fig. 1. (c) Measured spectral intensity (black) and retrieved phase (thick red line, with the standard deviation indicated by thin red lines). (d) Retrieved electric field of the pulses for the BK7 wedge insertion that minimizes the intensity FWHM duration, corresponding to a 3.8 fs pulse.

### *3.5 Pulse compression optimization*

Despite the achieved 1.6-cycle pulses, there is a significant difference between the transform-limited duration of the spectrum and the measured duration (from 2.9 fs to 3.8 fs, a 31% increase), mainly due to residual TOD (approximately –40 $fs^3$). Additionally, this TOD creates several post-pulses (Fig. 5(d)), which take a significant amount of energy away from the main pulse. Clearly, a small TOD adjustment would increase the peak intensity as well as shorten the pulse duration below the 1.5-cycle regime, both improvements greatly desirable for strong field physics experiments.

The first possible solution to this problem would be to design and fabricate chirped mirrors with a more adequate phase. This is, however, costly and time consuming. Another possible solution is to replace the BK7 wedges with a material with the appropriate GVD/TOD ratio such that the output phase of the hollow fiber plus the material propagation is perfectly compensated for by the bounces in the chirped mirrors, but the universe of available materials is limited and that would not add the degree of freedom one needs to account for possible variations in the hollow fiber output phase. Hence, besides the BK7 wedges, one can add another material such that by controlling its thickness the right GVD/TOD ratio can be obtained. Since we need to add TOD for a certain value of GDD, this means this material must have a lower GVD/TOD ratio than BK7 (<1.3 $fs^{-1}$). In order to find such material one can search through GVD and TOD values available in the literature for

#205337 - $15.00 USD Received 23 Jan 2014; revised 14 Mar 2014; accepted 25 Mar 2014; published 21 Apr 2014

transparent materials commonly available in optical laboratories (Fig. 6). Preferably, the choice should fall on common optical glasses or crystals, but those either have a similar or a higher GVD/TOD ratio than BK7. Air propagation also has a much higher ratio than BK7. Water, however, is ideal for this task, as it has a GVD/TOD ratio of 0.7 $fs^{-1}$ [19]. This way, one only needs to add approximately 2.5 mm of water and remove 1.35 mm of BK7 to add the required 40 $fs^3$ of TOD for the same value of GDD. Equivalently, one can keep the same BK7 insertion and add more chirped mirror bounces.

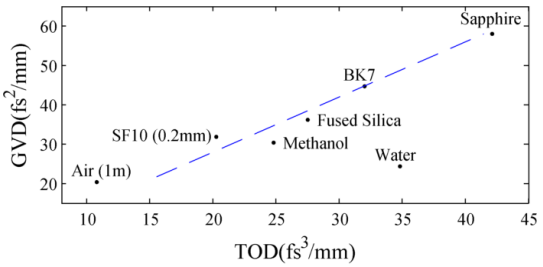


Fig. 6. GVD and TOD values at 800 nm for materials commonly available in optical laboratories; values for water taken from [19]. The GVD/TOD ratio of BK7 is represented by the blue dashed line.

This way, we added 4 more bounces off the chirped mirrors and used 4 mm of propagation through deionized water, which was the length of water that minimized the tilt in the trace. A typical resulting dispersion-scan trace is represented in Fig. 7, along with the retrieved scan and temporal and spectral analysis. We observe a clear increase in the quality of the compressed pulses compared to Fig. 5: shorter duration, higher intensity and reduced post-pulses. The retrieved pulse duration in these conditions was 3.2 ± 0.1 fs at a central wavelength of 722 nm, corresponding to a 1.4-cycle pulse. The relative intensity of the residual satellite pulses is reduced from 22% (Fig. 5(d)) to 10% (Fig. 7(d) – a 54% decrease.

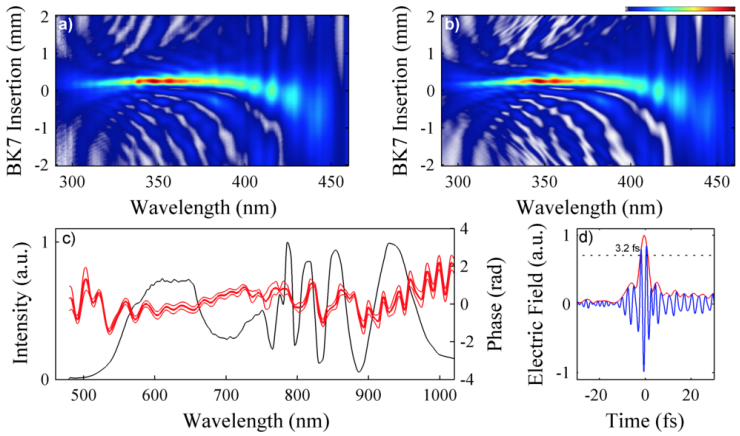


Fig. 7. Measured (a) and retrieved (b) d-scans for the setup in Fig. 1, with an additional 4 mm of propagation through water and 4 additional chirped mirror bounces. (c) Measured spectral intensity (black) and retrieved phase (thick red line, with the standard deviation indicated by thin red lines). (d) Retrieved temporal profile for the BK7 insertion that minimizes the intensity FWHM duration, corresponding to a 3.2 fs, 1.4-cycle pulse.

### *3.6 Measurement bandwidth analysis*

Due to the large bandwidth of these pulses it is important to assure that the bandwidth of the SHG/SFG crystal is sufficient to retrieve the phase over the whole spectrum. As noted in [11,14], the SHG of pulses with broad spectrum needs to be analyzed as intra-pulse SFG: all frequencies mix with each other, as long as they are compressed. Hence the signal at e.g. 400

#205337 - $15.00 USD Received 23 Jan 2014; revised 14 Mar 2014; accepted 25 Mar 2014; published 21 Apr 2014

nm is not only due to the SHG of the components at 800 nm, but also has information on the phase of all pairs of frequencies that SFG to 400 nm. These different SFG signals will interfere with each other and generate the different features of the d-scan trace.

In this work, the SFG signal was measured and retrieved between 290 and 450 nm. The signal above 450 nm was contaminated with a small amount of fundamental, hence was not usable. So one can argue that there is no SHG spectrum of the components outside the range of 580-900 nm, only SFG – e.g., signal from the mixing of 500 and 1000 nm will be located at 333 nm. This signal is enough to correctly retrieve the phase. In order to demonstrate that the measurement has information on the components outside the 580-900 nm range, one can do a simple calculation. If the measurement is indeed sensitive to the phase of the edges of the spectrum, then a small numerical perturbation introduced in this phase will change the shape of the corresponding d-scan trace, generating a trace with a larger error when compared to the measured trace. If the measurement is not sensitive, then one would expect no changes to the features of the trace and the error would be similar. This is demonstrated in Fig. 8. We considered a small temporal delay on the wavelengths above 950 nm (5 fs, Fig. 8(a), red curve) and the wavelengths below 550 nm (3 fs, Fig. 8(a), blue curve), which increased the pulse duration from 3.2 fs to 3.3 fs in both cases. We then calculate the error between measured and calculated traces: for the retrieved phase it is 0.7%, while for the 950 nm perturbation it is 2.4% and for the 550 nm one 2.2%. In order to visualize the change in the d-scan trace generated by perturbing the edges of the spectrum, we have represented the difference between the calculated traces and the measured one (Figs. 8(b), (c) and (d)). We see that a small change in the phase away from the center of the spectrum creates significant changes in the center of the d-scan trace, which makes it possible to retrieve the phase across the whole bandwidth.

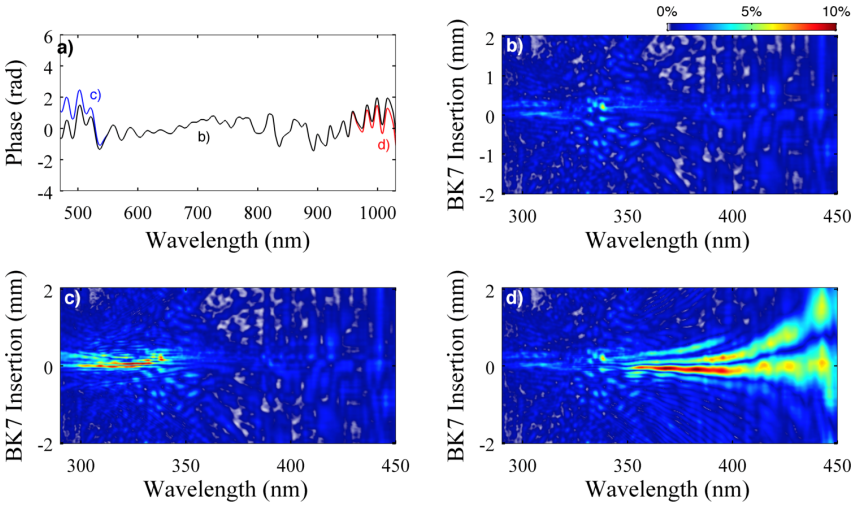


Fig. 8. Illustration of the SFG nature of the d-scan trace. a) Retrieved phase (black) and perturbed phases (5 fs delay above 950 nm – red; 3 fs delay below 550 nm – blue). b) Absolute difference between measured and calculated trace for the retrieved phase, scaled by the peak of the measured trace, corresponding to a total error of 0.7%. c) Similar to b) but for the phase perturbed below 550 nm. Features with more than 10% amplitude appear at the SFG wavelengths between the whole spectrum and the <550 nm components, corresponding to a total error of 2.3%. d) Similar to b) but for the phase perturbed above 950 nm, corresponding to a total error of 2.2%.

### *3.7 Carrier-envelope phase stabilization*

As mentioned previously, the dispersion–scan setup doubles as an f-2f interferometer. If used on a partial reflection of the main beam, it can serve for CEP monitoring and feedback, making it a single and complete solution for the generation and measurement of CEP-stable,

#205337 - $15.00 USD Received 23 Jan 2014; revised 14 Mar 2014; accepted 25 Mar 2014; published 21 Apr 2014

high energy few-cycle pulses. Due to the high reflectivity of the chirped mirrors at 450 nm it is possible to couple some of the fundamental beam into the spectrometer, along with the SHG, simply by opening the variable slit. In these conditions we immediately obtain low contrast but consistent f-2f fringes in the d-scan trace. By further optimizing the alignment for fringe contrast we can achieve a good signal from which the slow CEP drift introduced from the output of the oscillator to just after the chirped mirror compressor can be extracted. The corresponding error provides a feedback signal to the second (piezo-actuated) wedge in the d-scan setup for fast correction of the CEP drift.

Typical results are presented in Fig. 9, revealing a stability of 140 mrad over 100 minutes (measured at 50 Hz, 4 shots per spectrum - limited by the spectrometer minimum integration and data transfer times). Assuming the phase noise is at frequencies of 250 Hz or above, the phase stability would then be 280 mrad.

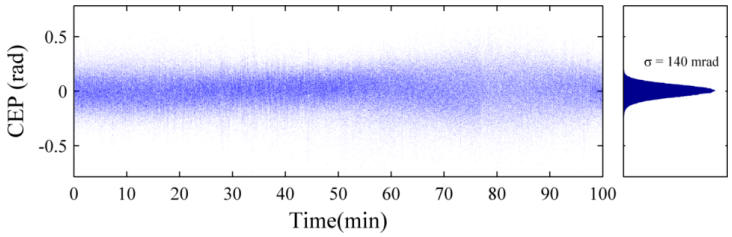


Fig. 9. CEP jitter evolution over 100 minutes, demonstrating a stability of 140 mrad (integrated over 4 shots).

## 4. Conclusion

In conclusion, we report on a convenient single setup for simultaneous dispersion compensation, temporal characterization and CEP stabilization of octave-spanning pulses in the single-cycle regime, based on post-compression of a standard CPA laser amplifier using an Ar-filled hollow-fiber and ultra-broadband double-angle chirped mirrors. The employed pulse characterization technique – d-scan – only requires adding a broadband SHG stage to the usual post-compression setup, and motorizing the dispersion and CEP adjusting elements (e.g., glass wedges). The resulting d-scan traces provide a powerful visual and analytical tool for optimization of both the chirped mirror angles and the residual TOD of the system, and the same d-scan setup allows measuring and stabilizing the CEP drift of the compressed pulses. Minimization of TOD by using a small propagation path in water resulted in 1.4-cycle, 3.2 fs pulses with 160 μJ (<0.5% rms) and a residual CEP jitter of 140 mrad over 100 minutes. The simplicity and robustness of the demonstrated d-scan based source and setup should be useful for strong-field applications and attoscience. Furthermore, the ability to measure the spectral phase over more than one octave hints at the possibility of using this technique to measure and characterize sub-cycle pulses over a broad range of frequencies, only limited by the bandwidth of the nonlinear process employed.

## Acknowledgments

This work was partly supported by FCT – Fundação para a Ciência e Tecnologia (PhD studentships SFRH/BD/37100/2007 and SFRH/BD/69913/2010, Post-Doctoral fellowship SFRH/BPD/88424/2012 and grant PTDC/FIS/115102/2009), co-funded by COMPETE and FEDER, the ESF - European Science Foundation (“Super-intense laser-matter interactions” grant 4596), Ministerio de Ciencia y Tecnología, Subdirección General de Proyectos de Investigación (Project FIS2009-07870) and the European Research Council (ALMA).